Published in "Advances in Colloid and Interface Science 235: 1–13, 2016"
which should be cited to refer to this work.

# Fractal-like structures in colloid science

S. Lazzari [a], L. Nicoud [b], B. Jaquet [b], M. Lattuada [c], M. Morbidelli [b,*]

[a] Department of Chemical Engineering, Massachusetts Institute of Technology, 77, Massachusetts Avenue, Cambridge, MA 02139, USA
[b] Institute for Chemical and Bioengineering, Department of Chemistry and Applied Biosciences, ETH Zurich, Vladimir-Prelog-Weg 1, 8093 Zurich, Switzerland
[c] Adolphe Merkle Institute, University of Fribourg,, Chemin des Verdiers 4, 1700 Fribourg, Switzerland

*Keywords:*
Fractal
Colloid
Materials
Cluster
Aggregate

A B S T R A C T

The present work aims at reviewing our current understanding of fractal structures in the frame of colloid aggregation as well as the possibility they offer to produce novel structured materials. In particular, the existing techniques to measure and compute the fractal dimension $d_f$ are critically discussed based on the cases of organic/inorganic particles and proteins. Then the aggregation conditions affecting $d_f$ are thoroughly analyzed, pointing out the most recent literature findings and the limitations of our current understanding. Finally, the importance of the fractal dimension in applications is discussed along with possible directions for the production of new structured materials.

**Contents**



* Corresponding author.
*E-mail address:* massimo.morbidelli@chem.ethz.ch (M. Morbidelli).

## 1. Introduction

Freely rephrasing Mandelbrot's words, nature exhibits fascinating geometrical patterns and shapes, which cannot be captured by Euclidian geometry. In order to be able to describe clouds, lightning, or the blood vessel architecture, a new mathematical instrument was developed, namely, fractal geometry. Ideal fractal objects are usually described as exhibiting self-similarity over an infinite range of length scales. In other words, the same geometrical pattern is identified over any scale one looks at fractals. Well-known examples for ideal fractals are the Koch snowflake and the Sierpinski triangle. On the other hand, there are natural fractals, which still exhibit self-similarity, but only on a limited number of scales: below their smallest repeating unit, no fractal scaling is observed. Among this category, one can find the most diverse objects, e.g., trees, lungs, river networks, and colloidal fractals.

Colloidal fractals are built-up starting from a colloidal suspension of primary particles aggregating in a finite-sized cluster. Note that henceforth, the terms “aggregate” and “cluster” will be used interchangeably as synonyms. It is worth recalling that most colloidal suspensions are only kinetically stable, in the sense that spontaneous (van der Waals forces-induced) aggregation of particles can only be delayed by an electrostatic or steric barrier, but eventually (i.e., thermodynamically) they will aggregate and phase separate from the continuous phase they were suspended into [1]. This implies that, in the vast majority of cases, fractal aggregates are non-equilibrium structures and are as such only kinetically stable. Other forms of structures obtained from the spontaneous organization of colloidal particles, such as colloidal glasses and colloidal crystals, the latter being stable equilibrium structures, are out of the scope of the present review [2].

It is accepted, since the work of Forrest and Witten [3], that large enough aggregates (or clusters) of colloidal particles follow a fractal scaling, i.e., their mass $i$ (that is their number of primary particles) scales with any characteristic cluster size, for example, the gyration radius $R_g$, according to a typically non-integer power law:

$$i = k\left(\frac{R_g}{R_P}\right)^{d_f} \tag{1}$$

where $R_P$ is the primary particle radius; $d_f$ is the fractal dimension of the colloidal aggregates, comprised between 1 (linear aggregates) and 3 (spherical aggregates); and $k$ is the fractal prefactor, a number which typically ranges between 1 and 1.2 and that has been reported to be a function of the fractal dimension itself [4,5]. A correlation providing a $d_f$-dependent prefactor, $k = k(d_f)$, has been proposed by Gmachowski [6]. Some of the colloidal fractals reported in the literature can be appreciated in Fig. 1. More details about the aggregation conditions and mechanisms are discussed in Section 3.

One should note that Eq. (1) holds for any characteristic size of the clusters, obviously with different values of the prefactor $k$. Several sizes have been used in the literature, including the hydrodynamic radius, the radius of the smallest sphere encompassing the cluster, the size of smallest box enclosing the cluster, etc. [5,10,11]. The radius of gyration is one of the most commonly used sizes because it is a purely geometrical property of the cluster and can be easily determined by static scattering methods. If the relative positions of the particles belonging to it are known, the radius of gyration can be computed from the following equation (valid for clusters made of identical primary particles):

$$R_g = \sqrt{\frac{1}{2N^2}\sum_{i,j=1}^{N}(r_i - r_j)^2} \tag{2}$$

where $N$ is the number of particles constituting the aggregate, while $r_i$ and $r_j$ are the positions of the $i$th and $j$th particles' centers. Although

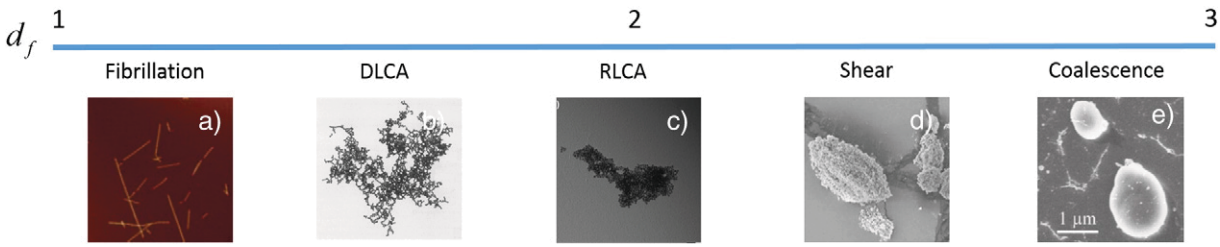


**Fig. 1.** Colloidal fractals exhibiting very different structures according to the aggregation conditions and mechanisms. (a) Protein fibrils [7]; (b) gold particles [8]; (c) gold particles [107]; (d) PMMA particles, ad hoc prepared; (e) rubbery polymer aggregates [9]. Fig. 1a), 1b), 1c) and 1e) are reprinted (adapted) with permission from their respective sources.

the notion of fractality applies only to sufficiently large clusters (of about 20 primary particles), it is worth mentioning that smaller-sized clusters also follow the mass scaling reported in Eq. (1), as was shown by Monte Carlo simulations [12].

The aim of this review is to discuss fractal-like structures in Colloid Science in the light of the most recent literature. In particular, first the available experimental and modeling techniques to study fractals will be discussed in terms of their applicability and limitation. Then the variables affecting $d_f$ will be analyzed in the frame of the three main phenomena occurring, namely, aggregation (particles "gather" to form clusters, also referred to as coagulation or flocculation [13]), breakage (clusters are broken in aggregates of smaller size), and coalescence (neighboring particles in the same cluster "fuse"). Finally, relevant applications, possible research directions and open challenges, will be pointed out, highlighting the role of fractal clusters in both the actual and future scenario.

## 2. Experimental and modeling techniques available to estimate the fractal dimension

In the present section, the experimental and modeling techniques to evaluate the clusters $d_f$ are briefly presented, highlighting the limits and advantages of each methodology. For a more detailed description of the techniques and protocols, which are out of the scope of the present review, the reader is referred to specific reviews and books on the topic [14–18].

### 2.1. Experimental techniques

A synoptic picture of the available experimental techniques, along with their typical applicability ranges in terms of initial occupied volume fraction $\varphi_0$ and primary particle diameter $d_p$, is reported in Fig. 2.

#### 2.1.1. Scattering techniques

*2.1.1.1. Measurement type.* Static light scattering (along with neutron or x-ray scattering) allows one to recover precious information about the structure of clusters. Most of the theory developed for the interpretation of the scattered intensity profile has been developed under the Rayleigh–Debye–Gans assumption, which is valid under the following conditions [18]:

$$\frac{2\pi \cdot n \cdot a_p}{\lambda_0} \cdot \left|1-\frac{n_p}{n}\right| \ll 1 \qquad \left|1-\frac{n_p}{n}\right| \ll 1 \tag{3}$$

where $\lambda_0$ is the in vacuo wavelength of the incident source, $n$ is the refractive index of the continuous medium, and $n_p$ is the refractive index of the particles. The two conditions mean that particles need to be smaller than the wavelength of the incident radiation and made of a material with a sufficiently low optical contrast compared to the continuous medium surrounding the particles. Under these conditions, and provided that a cluster is made of identical primary particles, the intensity of scattered light as a function of the scattering angle takes the form:

$$I(q) \approx S(q) \cdot P(q) \tag{4}$$

$I(q)$ is the intensity of the scattering light, which is decomposed into the product of two terms: the scattering structure factor $S(q)$ and the particle form factor $P(q)$. The former contains information about the structure of the cluster, while the latter about the size and shape of the primary particles. The scattering wave vector $q$ [$m^{-1}$] is defined as

$$q = \frac{4\pi n}{\lambda_0} \sin\left(\frac{\theta}{2}\right) \tag{5}$$

where $\theta$ is the scattering angle (i.e., the angle between the incident beam and the direction of observation). The scattering structure factor is related to the relative positions of the particles in the clusters. This information is provided by the particle–particle correlation function, $g(r)$, which represents the average number of particles located at a distance $r$ from the average particle in the cluster. The scattering structure factor is the spatial Fourier transformation of the particle–particle correlation function [14]:

$$S(q) = 1 + 4\pi \int_0^\infty g(r) \frac{\sin(q \cdot r)}{q \cdot r} r^2 dr \tag{6}$$

The scattering structure factor of a cluster can be divided into three different regions. The first one, for sufficiently low values of the scattering wave vector, is the so-called Guinier regime, from which the radius of gyration of a cluster can be determined. The second region is the fractal regime, characterized by a power law, while the third one is the individual particle regime. The cluster fractal dimension $d_f$ can be obtained from the scattering structure factor in essentially two different ways. The first one is based on plotting in double logarithmic coordinates the structure factor $S(q)$ against the scattering wave vector. Recalling that for fractal objects in the fractal regime [18],

$$S(q) \propto q^{-d_f} \tag{7}$$

it is clear that from the log–log plot of $S(q)$ *vs* $q$ the clusters $d_f$ is found. This holds only if the $q^{-1}$ range investigated lies between the overall aggregate size (e.g., described by the gyration Radius $R_g$) and the primary particles radius, $R_p$ i.e., [14]:

$$R_g \gg q^{-1} \gg R_p \tag{8}$$

Eq. (7) relies on the assumption that the particle–particle correlation function also shows a fractal scaling:

$$g(r) \propto r^{d_f - 3} \tag{9}$$

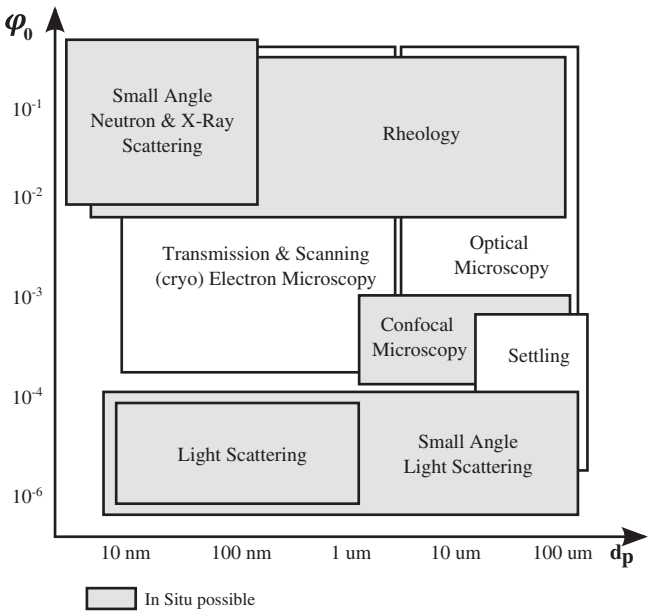


**Fig. 2.** Available experimental techniques. Initial occupied volume fraction $\varphi_0$ and primary particle diameter $d_p$ set the utilization boundaries.

In order to obtain a reliable estimate of the fractal dimension from Eq. (7), it is necessary that the self-similarity of the clusters covers a sufficiently large range of length scales; otherwise, the slope estimated is not well defined. Additionally, the value of the fractal dimension can be affected by a strong polydispersity of the cluster population [16].

The second possibility requires plotting the $I(0)$ (scattered intensity extrapolated at $q=0$) versus $R_g$ in a log–log plot. Once more, the slope gives the $d_f$ [19], according to the following equation:

$$I(0) \propto \left(\frac{R_g}{R_p}\right)^{d_f} \tag{10}$$

Employing the latter equation is possible if the intensity can be measured for clusters populations with different average sizes, as it happens when the kinetics of aggregation is monitored. The key difference as compared to the first methodology is the required $q$ range: in the latter case, the limitations given by Eq. (8) do not apply, as $R_g$ can be estimated from the Guinier plot (or Guinier regime), at relatively small $q$, such as $q^{-1} \approx R_g$, according to the following equation:

$$S(q) = 1 - \frac{1}{3}q^2 R_g^2 + \ldots \tag{11}$$

In this case, the small $q$ range of the scattering structure factor needs to be experimentally accessible.

*2.1.1.2. Characteristic of the cluster dispersion.* Scattering techniques can be applied to colloidal suspensions of very different sizes, ranging from 10 nm to 10 μm, hence covering the whole colloidal range (cf. Fig. 2) by tuning the wavelength $\lambda_0$ (achieved for instance by choosing between light, neutron or x-ray scattering) and the scattering angle $\theta$ appropriately [14]. For the measurement to be effective, the particle concentration should be lower than about $\phi = 10^{-4}$ in order to avoid multiple scattering. Moreover, a difference between the refractive indices of the continuous and dispersed phase should exist so that the laser source is scattered and not simply refracted [20]. More precisely, the interplay between refractive index and occupied volume fraction is key: samples with $\phi > 10^{-4}$ may be analyzed, provided the difference between their refractive index and the one of the continuous medium they are suspended into, is sufficiently small [20].

*2.1.1.3. Advantages and limitations.* Among the perks of employing scattering techniques, both the good statistical relevance of the measurement and the non-destructiveness of the technique ought to be mentioned. As a drawback instead, it should be recalled that the aggregate information are obtained through indirect measurements. More explicitly, the Rayleigh–Debeye–Gans theory relates the scattered intensity to the clusters size, form, and structure. Limitations of the employed theory might clearly affect the obtained results in specific cases [20].

*2.1.2. Microscopy techniques*

*2.1.2.1. Measurement type.* From microscopy pictures, it is possible to estimate the fractal dimension of clusters by plotting (in log–log) the mass of each cluster (i.e., the number of particles constituting it) versus their measured radius. (cf. Eq. (1)) This holds both for 2D pictures (from optical, atomic force, scanning electron and transmission electron microscopy, OM, SEM, and TEM) as well as for the 3D reconstruction available through confocal microscopy (CM) [14].

*2.1.2.2. Characteristic of the clusters.* Specific size limitations apply for different microscopy techniques, but roughly it can be stated that optical microscopy cannot resolve clusters smaller than 500 nm, whereas AFM, SEM, TEM, and CM have a much smaller limit (about 10 nm). In all cases, the analyzed samples should be diluted enough to avoid clusters overlapping. Moreover, the clusters $d_f$ should be smaller than 2, as it is necessary to assume that the measured $d_f$ (coming from a 2D projection) corresponds to the real, 3D one. The latter issue holds only for 2D pictures, as CM allows resolving a complete 3-D picture of the cluster [14]. However, even in the case of dense clusters, with a fractal dimension higher than 2, from the projection, it is possible to estimate a perimeter fractal dimension, which can be related to the real fractal dimension through known correlations [21,22].

*2.1.2.3. Advantages and limitations.* The main advantage of microscopy techniques is that a direct visualization of the aggregates (and hence of their spatial organization) is possible. A further perk of these measurements is that they represent the only experimental possibility to estimate the fractal prefactor $k$ (cf. Eq. (1)). Moreover, the microscopy techniques that involve a freezing step (cryo SEM/TEM) allow one to analyze the dispersion directly, with no further sample manipulation (e.g., drying). On the other hand, to obtain meaningful statistics, several hundred (ideally thousands) clusters should be processed, resulting in a time-consuming operation, especially when compared to the available automation level of light scattering techniques.

*2.1.3. Rheology*

*2.1.3.1. Measurement type.* At high particle concentrations, aggregating systems may organize in so-called colloidal gels. A colloidal gel is a network whose components consist of fractal clusters, which in turn are made of colloidal particles [23,24].

The $d_f$ measurement from rheological experiments requires to process a colloidal gel in a rheometer, to obtain the plateau storage modulus $G'$. With an appropriate model, correlating $G'$ to the gel's structure organization, it is possible to obtain information regarding the fractal dimension $d_f$ of the blobs forming the gel. Different formulas have been proposed according to the nature of the primary particles constituting the colloidal gel (e.g., proteins or polymer particles) [15,24]. A qualitative equation, underlying the dependency of $G'$ from the occupied volume fraction and a generic fractal dimension function $f(d_f)$, reads

$$G' \propto \varphi^{f(d_f)} \tag{12}$$

The expression for $f(d_f)$ changes according to the interactions of the flocs constituting the gel. In particular, three different "gel regimes" are identified, a strong-link regime, where interfloc links are stronger than intrafloc links, a weak-link regime, where the opposite is true, and an in-between case, referred to as transition regime [24]. The parameter $\alpha \in [0,1]$ allows to move from the strong-link regime ($\alpha = 1$) to the weak-link regime ($\alpha = 0$) through the transition regime (where $\alpha$ has intermediate values). $f(d_f)$ reads:

$$f(d_f) = \frac{(d-2) + (d+x)(1-\alpha)}{d - d_f} \tag{13}$$

where $d$ is the Eucledian dimension of the system considered and $x$ is the fractal dimension of the gel backbone [24]. Notably, using Eq. (12) implies assuming that gels obtained from differently concentrated suspensions lead to the same fractal dimensions. In practice, this requires performing experiments over a narrow range of volume fractions.

*2.1.3.2. Characteristic of the cluster dispersions.* The colloidal samples that can be analyzed by rheological measurements are limited to colloidal gels, as no $G'$ can be defined for a liquid-like sample.

*2.1.3.3. Advantages and limitations.* The present technique has two major advantages, namely, it allows to link macroscopic properties of a gel with the aggregates structure, and it is "orthogonal" as compared to scattering and microscopy techniques. As a matter of fact, it allows

analyzing highly concentrated samples in the gelled state, which are otherwise difficult to process.

### 2.2. Modeling techniques

#### 2.2.1. Monte Carlo techniques

*2.2.1.1. Simulation type.* Monte Carlo models follow the structural evolution of an aggregating colloidal system [25]. Typically, a given number of primary particles is randomly placed in a 3-D lattice and allowed to move and "react" according to specific rules and probabilities. At the end of the simulation, a population of clusters with given structures is obtained; employing Eq. (1), it is possible to estimate both the $d_f$ as well as the fractal prefactor $k$. Notably, different aggregation conditions (e.g., allowing only particle–cluster interactions) or the impact of differently sized primary particles can be investigated using Monte Carlo techniques, which prove in this sense their versatility [26].

*2.2.1.2. Advantages and limitations.* Monte Carlo techniques are computationally efficient (they can be used to simulate systems containing up to $10^6$ particles) and provide in a very direct way the structural properties of a given aggregation condition. On the other hand, in Monte Carlo simulations the time evolution is described in a somehow artificial manner, so that extracting kinetics information is not at all trivial. For this reason, Monte Carlo does not allow describing those structural evolutions, which are affected by the rates of interplaying kinetic processes (e.g., simultaneous aggregation and coalescence, restructuring), nor it provides a time-dependent evolution of the $d_f$ but rather a "steady-state picture" [25]. An additional limitation of Monte Carlo simulations is that it is not trivial to simulate aggregation processes that involve interactions that cannot be described by potential functions, such as hydrodynamic effects (e.g., shear-induced aggregation, hydrodynamic interactions, etc.).

#### 2.2.2. Molecular dynamics, Brownian dynamics, and Stokesian dynamics

*2.2.2.1. Simulation type.* Both Brownian and Stokesian dynamics simulations provide a full description of the particles motion by solving the Langevin equation [27–29]. The overdamped form of Langevin Equation for the generic $i$th particle in a system with $N$ particles, where particle inertia is neglected, is the following:

$$f_i \cdot \mathbf{v}_i = \mathbf{F}_i + \sum_{j \neq i}^{N} \mathbf{F}_{i,j} + \mathbf{F}_{B,i} \tag{14}$$

where $f_i$ is the friction factor of the $i$th particle, $\mathbf{v}_i$ the particle velocity, $\mathbf{F}_i$ is the external force acting on the $i$th particle, $\mathbf{F}_{i,j}$ is the interparticle force exerted by particle $j$ on particle $i$, and $\mathbf{F}_{B,i}$ is the Brownian stochastic force acting on the $i$th particle. The key difference between Brownian and Stokesian dynamics is that in the latter hydrodynamic interactions among particles are rigorously accounted for. These techniques treat the solvent as a continuum and consider it only implicitly, typically through the addition of stochastic forces. All structural information about the clusters are available, including $d_f$ and the fractal prefactor $k$, which can be estimated through Eq. (1) knowing the number of particles building up the cluster and its radius.

Molecular dynamics, based on the solution of Newton's laws of motion, instead deals with the solvent explicitly, by directly considering the interactions of the particles with the solvent molecules [25]. Since molecules need to be explicitly accounted for, molecular dynamic simulations are not suitable to follow aggregation processes, because only very few particles can be included in the simulation box. However, complex processes such as sintering or coalescence of a few particles can be simulated [30]. Therefore, the results of these simulations can be used to validate macroscopic models, as they provide insights on complex processes (such as sintering or coalescence), which induce a change in the fractal dimension. This becomes of particular relevance when modeling the simultaneous aggregation and coalescence of a colloidal system, where a time-dependent expression for the fractal dimension is necessary to properly account for the interplay of the two phenomena [30].

*2.2.2.2. Advantages and limitations.* Brownian and Stokesian dynamics are able to account for virtually any type of effect (e.g., hydrodynamic forces, electrostatics, etc.) in a quite rigorous way, while giving the user a direct, fully detailed view of the on-going cluster formation. The key drawback for such simulations is the significant computational time, which leads to lengthy simulations [25].

#### 2.2.3. Population balance equations

*2.2.3.1. Simulation type.* Population balance equations, i.e., a set of coupled ordinary differential equations (ODEs), allow to deterministically describe the time evolution of aggregating systems, solving the Smoluchowksi Equation [4]:

$$\frac{dN_k}{dt} = -N_k \sum_{j=1}^{\infty} \beta_{j,k} N_j + \frac{1}{2} \sum_{j=1}^{k-1} \beta_{k-j,j} N_{k-j} N_j \tag{15}$$

where $N_k$ is the concentration of clusters of size $k$ and $\beta_{j,k}$ represents the aggregation rate (also referred to as kernel) between two clusters of sizes $j$ and $k$. Typically, discretization techniques are employed to reduce the size of the problem from $10^4$–$10^5$ (ODEs) to about $10^2$ equations [31,32]. The aggregation kernels employed are usually a function of the aggregating clusters $d_f$, as exemplified here with the diffusion-limited cluster aggregation kernel [4]:

$$\beta_{j,k} = \frac{2k_B T}{3\eta_C} \left( j^{1/d_f} + k^{1/d_f} \right) \left( j^{-1/d_f} + k^{-1/d_f} \right) \tag{16}$$

where $T$ is the temperature, $k_B$ is the Boltzmann constant, and $\eta_C$ is the viscosity of the continuous phase. Note that $d_f$ is estimated by comparing the model predictions with experimental data sets (e.g., average hydrodynamic and gyration radii) [10,12].

*2.2.3.2. Advantages and limitations.* Population balance equations are usually easily solved, provided that the number of internal coordinates (e.g., cluster mass, fractal dimension, etc.) is kept low (typically 1–2). They allow following time-dependent restructuring phenomena and provide a quantification of the influence of the $d_f$ on the aggregation kinetics or cluster size distribution. As downsides, it has to be recalled that suitable kernel expressions have to be found for the different cases analyzed (no universal kernel exists). Moreover, experimental information has to be available in order to test the kernel's soundness against a measurable quantity. This type of comparison is therefore indirect and provides a tool for describing a given phenomenon (e.g., simultaneous aggregation and breakage or restructuring) rather than a methodology to identify the corresponding mechanism.

## 3. Processes affecting the cluster fractal dimension

In the present section, the processes defining the $d_f$ of colloidal clusters are identified and discussed, in an attempt to provide a critical picture, pointing out literature inconsistencies. The impact of the variables controlling such processes (i.e., aggregation, breakage, and coalescence) is discussed.

### 3.1. Aggregation

#### 3.1.1. Interaction potential

The aggregation of colloidal particles is regulated by the balance between repulsive and attractive forces, or rather by the corresponding

repulsive ($V_R$) and attractive ($V_A$) potentials. In the classical case referred to as DLVO (Derjaguin–Landau–Verwey–Overbeek) systems, these correspond to electrostatic and van der Waals interactions, respectively.

By regulating the total potential, $V_T = V_A + V_R$, it is possible to modify the aggregation rate. As a matter of fact, if no repulsive forces are present, the colloidal particles aggregate, in stagnant condition, upon contact. This process is the so-called diffusion-limited cluster aggregation (DLCA). On the other hand, when a repulsive potential is in place, only a fraction of the occurring collisions is effective (as not all particles overcome the repulsive forces present), and one speaks of reaction-limited cluster aggregation (RLCA) [20]. To compare the total potentials against particle distance in the two cases, consider Fig. 3a). The universality of these two aggregation regimes has been demonstrated for several types of colloidal particles [33].

*3.1.1.1. Repulsive forces.* The two different aggregation regimes, DLCA and RLCA, give rise to clusters having different $d_f$. Open clusters are formed in DLCA aggregation as the particles stick upon contact, while more compact clusters are found in RLCA aggregation as several collision events have to occur (due to the repulsive potential) before the clusters stick together. The electrostatic repulsive barrier is affected by the particles surface composition (e.g., adsorbed surfactants) and by the interaction between the particles surface and the dispersant (where pH and salt concentration may significantly affect the repulsive barrier). Monte Carlo and Brownian dynamics simulations indicated that clusters formed in the DLCA regime have a $d_f \approx 1.8$, while RLCA forms aggregates having $d_f \approx 2.1$ [34–36]. Experimental evidences of the transition between the two regimes as a function of the stability ratio showed how the $d_f$ monotonically increases with the stability ratio [37]. While this description is fairly accepted in the literature, its validity is usually restricted to diluted systems of monodisperse, charge-stabilized primary particles, undergoing stagnant homo-aggregation. The plot thickens when the complexity of the colloidal system analyzed increases; long-range attractive forces, high particle concentrations, polydispersed particles, and patchy particles give rise to significant deviations from the "idealized" picture mentioned above. In the next sections such deviations are summarized, highlighting the most recent and relevant literature contributions in this direction.

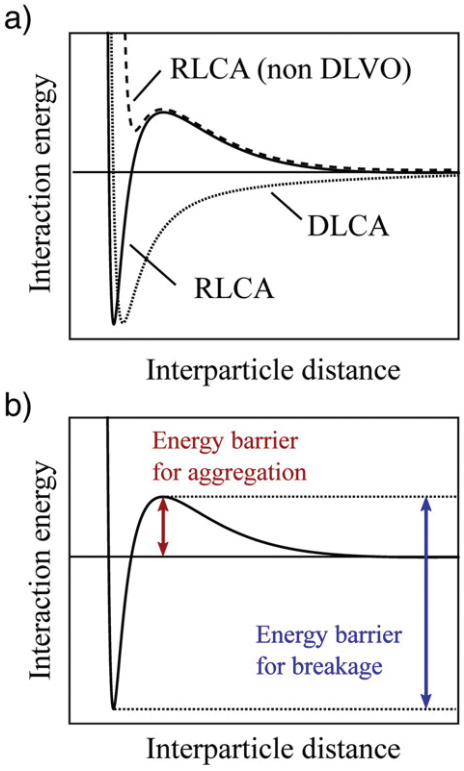


**Fig. 3.** (a) interaction potential for DLCA (dotted line), RLCA (continuous line), and non-DLVO RLCA (dashed line). (b) Total interaction potential highlighting the energy barrier to be overcome in the cases of aggregation and breakage.

In the case of aerosols, even in the absence of interactions among particles, the mechanism of cluster formation is different from that of particles aggregating in a liquid suspension [4,38]. Aerosol particles typically move in the so-called free molecular regime. The latter regime is caused by the high temperatures in the aerosol reactors [4] and the resulting low density of the gas phase, which leads to a low friction experienced by particles, whose trajectories become almost rectilinear. The corresponding aggregation mechanism, called ballistic aggregation, leads to somehow denser clusters than in the case of diffusion-limited aggregation, with typical cluster fractal dimension values of around 1.9 [38]. Computer simulations confirmed these experimental findings. Additionally, it has also been verified through simulations that, when the density of the gas increases, a transition happens from ballistic to diffusion-limited aggregation (where particle motion becomes diffusive following Epstein diffusion) [39].

*3.1.1.2. Attractive forces.* Interestingly, the presence of further attractive interactions apart from van der Waals forces may affect the clusters $d_f$. For instance, when studying the heteroaggregation of oppositely charged polystyrene particles, long-range attraction forces lead to fractal dimensions as low as 1.2; hence, worm-like clusters were formed. Upon increase of the ionic strength of the medium (hence screening the opposite surface charges), more compact structures closer to the DLCA limit were found. By properly tuning the salt concentration, it was therefore possible to create fractal structures with very diverse branching degrees [40].

Depletion interactions are another example of attractive interactions often used to induce controlled self-assembly of particles [41]. Depletion interactions are generated by the addition of polymers or smaller particles to a suspension of colloidal particles. A further possibility to induce depletion interactions is represented by the addition of surfactants in concentrations larger than their critical micellar concentration. In these cases, a somewhat counterintuitive role of the surfactants emerges: if added beyond a certain amount, their stabilizing effect (through adsorption on the particles to be stabilized) turns into a strongly destabilizing effect caused by micelles-induced depletion forces [42]. One of the most investigated systems consists of crosslinked PMMA particles dispersed in a mixture of cis-decaline and cyclohexyl bromide, and polystyrene chains are used as depleting agent. The mixture of solvents is chosen so as to match both the refractive index and the density of the particles. This way, van der Waals interactions and sedimentation effects are both minimized. With depletion interactions, both the depth and the range of attractions can be fine tuned. Colloidal particles subject to depletion interactions form clusters with fractal dimension values depending on the range of attractive interactions. In the case of long polymer chains, very high fractal dimension values of about 2.4–2.6 are reported, while short polymer chains lead to the formation of clusters with fractal dimension values similar to those of DLCA. Intermediate polymer chains lead to intermediate values of fractal dimensions [41].

*3.1.2. Dipolar interactions*

Magnetic particles experience dipolar interactions either in the presence of a magnetic field, which causes them to align into chain-like structures, or, when they behave as permanent magnetic dipoles, even in the absence of magnetic fields [43–45]. De Gennes and Pincus were the first to demonstrate that dipolar interactions lead to clusters with a fractal dimension of about 1.2 [46]. Among the structures observed in the case of magnetic particles, the presence of closed chains, so-called loop clusters, has been demonstrated both experimentally and though simulations [47]. Even charged particles, when subject to alternating electric fields, develop dipolar interactions, which guide them into

chain-like structures [48]. Depending on the strength of the dipolar interactions compared to the scrambling effect of Brownian motion, the fractal dimension of the chains can vary between 1 and 1.2. [47].

*3.1.3. Primary particle concentration*

Monte Carlo studies investigating the increase in primary particle concentration (hence in the initial occupied volume fraction $\varphi_0$) reported the formation of rather compact clusters, exhibiting $d_f$ in DLCA regime ranging between 1.8 ($\varphi_0 \to 0$) and 2.5 ($\varphi_0 \approx 0.5$), hence significantly larger than the typically reported values, of about 1.8. The dependency of $d_f$ on $\varphi_0$ was reported to be approximately of square root type. Such an increase in $d_f$ was ascribed to cluster collisions occurring close to the cluster centers rather than at their tips due to increased $\varphi_0$ [49]. A similar trend has been observed generating colloidal gels in DLCA and RLCA conditions through Monte Carlo simulations; the gels $d_f$ were shown to increase upon increasing the initial occupied volume fraction in the range $\varphi_0 = 0.01 - 0.08$ [50]. An experimental confirmation was recently reported in the field of antibody aggregation [51]: at larger initial protein concentration, an increase in fractal dimension was observed, following the scaling suggested by the aforementioned study [49]. In this frame, more experimental evidences would be of help to confirm if and to which extent the observed trends hold also for other colloidal systems and in different experimental conditions.

*3.1.4. Primary particle size*

Recently, another deviation from the "ideal behavior" of fractal structures in the DLCA regime was reported [50]. In particular, it turned out that the fractal dimension of the formed clusters is a function of the particle size: small primary particles (radii of about 10 nm) lead to the commonly accepted fractal dimension $d_f \approx 1.85$, while larger primary particles (radii in the order of $150 - 200$ nm) cause fractals to be less compact, with $d_f$ values as low as 1.6. This result was obtained by revising a significant amount of literature data involving colloidal suspension of various types (e.g., polystyrene, silica, hematite) and performing ad hoc experiments with differently sized polystyrene particles [50]. This intriguing observation (of $d_f$ depending on the particles radii) still requires a theoretical explanation: it has been suggested that small dipolar interactions could be at the root of the phenomenon, but in the absence of a proper theoretical framework, this hypothesis could not be confirmed. A further interesting question is whether a comparable situation arises in the RLCA regime or this remains a peculiarity of DLCA aggregating clusters.

*3.1.5. Primary particles polydispersity*

Particle polydispersity has a significant effect on the fractal dimension of aggregating clusters. Eggersdorfer and Pratsinis [26] showed that a quite polydispersed colloidal suspension (with a geometric standard deviation $\sigma_g \to 3$) leads to quite open clusters with $d_f \to 1.5$ disregardful of the aggregation regime considered (e.g., DLCA, diffusion-limited aggregation (DLA) and ballistic particle–cluster aggregation (BPCA)). Note that the typical $d_f$ for DLCA, DLA, and BPCA are considerably larger (i.e., 1.8, 2.25 and 2.81, respectively), underlining the strong impact of polydispersity on $d_f$. Interestingly, such low $d_f$ values arise only for large enough polydispersities, whereas for rather monodisperse systems ($\sigma_g \approx 1 - 1.5$), "standard" values for $d_f$ were found, as already observed in the Monte Carlo studies of Bushell and Amal [52] for DLCA and by Tence et al. in BPCA [53]. It should be stressed though that this interesting dependency of $d_f$ from the particles polydispersity has been observed only in simulations, and that it would be of great interest to seek for an experimental confirmation. A further step toward the understanding of the polydispersity relevance could be to verify if and how this phenomenon is affected by the particle concentration, whose increase has been reported to increase $d_f$, as discussed earlier in paragraph 3.1.3.

*3.1.6. Two-dimensional aggregation*

While most of the studies on aggregation of colloids have been performed on three-dimensional systems, aggregation in two dimensions has also been investigated [54–57]. A 2-D aggregation was studied by computer simulations in the eighties because of the lower computational time required. For the ideal diffusion-limited and reaction-limited aggregation, the fractal dimension values are 1.46 and 1.55, respectively [56]. Two-dimensional aggregation has been experimentally investigated by trapping particles at interface between a liquid (usually water) and a gas (typically air), or by drying particles on a surface [55,58]. Experimental results match the results of Monte Carlo simulations. However, the interactions between two particles at the air–water interface are highly complex. In addition to electrostatic interactions acting on the portion of particles submerged in water, electric dipoles develop on the portion of particle surface exposed to air [55]. Furthermore, capillary forces are also acting because of the deformation of the air–water interface caused by the presence of the particles. While the electrostatic interactions in aqueous phase can be screened by increasing the ionic strength, the other interactions remain relatively long-ranged.

*3.1.7. Bridging flocculation*

Bridging flocculation is a common aggregation mechanism, heavily utilized in wastewater treatment, where flocculants, very often cationic polymers, are added to a suspension of particles to be flocculated [59]. The long molecular weight polymer chains tend to attach to multiple particles, inducing aggregation by bridging them. The clusters formed under these conditions are open, with a fractal dimension of about 1.6–1.7, slightly lower than those found in DLCA [60]. However, in practically relevant conditions, this aggregation process is carried out in the presence of shear, which as expected increases the density of clusters, and therefore their fractal dimensions, to values ranging from 2.4 to 2.8, depending on the shear rate used [61]. It is generally observed that clusters obtained from bridging flocculation have lower fractal dimension than the one formed from their counterparts obtained by just addition of high concentration of electrolytes under otherwise identical conditions [62].

*3.1.8. Sedimentation*

Sedimentation is another mechanism affecting the structure of clusters formed when colloidal particles are colloidally unstable. The effect of sedimentation is to increase the cluster fractal dimension since large clusters settle faster than small clusters, and then to capture them in their motion. Monte Carlo simulations, performed under the assumptions that clusters remain rigid and that hydrodynamic interactions are negligible, showed that the fractal dimension of clusters obtained by fully destabilized particles in the presence of gravity is close to 2.1 [63,64]. Few experimental data are available in the literature, which point to similar results, or even to higher fractal dimension values, most probably due to some intrinsic restructuring of the clusters [65].

*3.2. Breakage*

Cluster breakage, typically occurring under shear conditions, causes the rupture of aggregates to form two smaller-sized clusters. The energy required for this fragmentation is a function of both the cluster structure (i.e., its $d_f$) and the primary particles surface properties. For instance, the energy required to break a doublet is the difference between the potential primary minimum and the stabilization maximum (cf. Fig. 3b) as recently clarified by Conchuir and Zaccone for DLVO potentials [66]. For larger clusters instead, it is not merely a question of breakage energy required but also of number of neighboring particles. In fact, reiterated aggregation and breakage events lead to cluster restructuring (compacting the clusters) and increase the number of particle contacts, therefore decreasing the breakage probability. Another view is given by discrete element method (DEM) simulations: it was shown that under shear, aggregates are stretched up to the point they break into

fragments that typically relax in more compact structures, to reduce their exposed surface to shear [67]. Notably, the $d_f$ values reached in this frame are larger than those observed in stagnant conditions reaching values in the range of 2.4–2.7 [68]. The lower limit of such range, i.e., $d_f = 2.4$, has been recently supported through a mathematical model providing analytical predictions of the aggregate $d_f$ during the aggregation process [69].

Breakage can occur also in stagnant conditions. In these cases, one often speaks of reversible aggregation, which is relevant in situations where the depth of the energy minimum in which particles find themselves when they aggregate is shallow [70]. Under this condition, spontaneous breakage of bonds might occur, thus leading to rearrangement of clusters. Therefore, cluster with higher fractal dimensions and higher number of nearest neighbor particles are formed. Typical values of fractal dimension increase as the depth of the energy minimum decreases, reaching values higher than 2.5 [71]. Computer simulations studies based on Monte Carlo methods have paved the way to explain the behavior of such systems, before experimental data where available [38].

Experimental data on reversible aggregation are difficult to obtain, since controlling the depth of the energy barrier is not an easy task. Experiments on gold nanoparticles with low concentrations of surfactants have been performed, which confirm the reversibility of the aggregation, as modeled by DLVO theory [70]. Soft particles, such as microgels, also show similar behavior. In this case, the reversibility is due to the soft hydrophilic polymer shell surrounding the particles. The measured fractal dimension values of microgel clusters formed under diffusion-limited conditions were found to be higher than those of rigid particles, with values approaching 2.1 [71].

The aforementioned picture represents a brief description of the breakage mechanism and its interplay with $d_f$; in the next sections the key parameters affecting such dependency are discussed in the frame of the most recent literature findings.

#### 3.2.1. Interaction potential

Given that the strength of a cluster regulates its propensity to undergo breakage (therefore affecting the cluster shape), it is clear that regulating or changing the particle interaction potential, especially at low separation distances, strongly affects the breakage process. Non-DLVO potentials are particularly interesting in this respect, as they sometimes lead to the absence of potential wells, thus changing the aforementioned picture. The yet unraveled interplay between potentials and cluster structures finds here one of its practical outcomes: the non-possibility to predict the type of breakage and thus the resulting fractal structure for non-DLVO stabilized particles. Recent work based on Stokesian dynamic simulations has however demonstrated that the structure and mass distributions of fragments generated by shear-induced breakage is virtually independent of the depth of the energy well existing between particles in a cluster [72].

#### 3.2.2. Shear rate, primary particle size

The cluster size history in aggregation-breakage processes is regulated by two key non-dimensional quantities, the Peclet number (Pe) and the Fragmentation number (Fa). Pe represents the ratio of the convective transport rate (i.e., the shear) and the diffusive transport rate (here represented by the particles thermal energy). Fa describes the ratio of the viscous shear stress to the strength of the clusters. The latter quantities read

$$\mathrm{Pe}_{i,j} = \frac{3\pi\eta_C\dot{\gamma}R_iR_j(R_i+R_j)}{2k_BT} \tag{17}$$

$$Fa_j = \frac{\eta_C\dot{\gamma}}{T_{S,j}} \tag{18}$$

where $\eta_C$ is the viscosity of the continuous phase, $\dot{\gamma}$ is the shear rate, $R_i$ the radius of an $i$-sized cluster, $T$ the temperature, $k_B$ the Boltzmann constant, and $T_S$ the characteristic cohesive strength of the aggregate [73]. Note that the cohesive strength is typically inversely proportional to the cluster radius, $T_S \propto R_j^{-1}$ or $T_S \propto R_j^{-0.5}$, according to the fragmentation mechanism being fracture at plane or crack growth, respectively [73]. Besides the temperature (which will be discussed in the next section) and the viscosity of the continuous phase, defined once $T$ and $\varphi_0$ are fixed, two main parameters influence both the Pe number and the Fa number: the shear rate $\dot{\gamma}$ and the cluster radius $R_i$. Accordingly, the interplay of aggregation and breakage in shear depends strongly on these parameters that clearly affect the resulting cluster $d_f$. An aggregate-stability map, discriminating between clusters restructuring and breakup as a function of the parameters $d_f$, $R/a$, and $\dot{\gamma}$ (fractal dimension, cluster size over primary particle radius and shear rate), has been recently presented [69]. Further efforts in this direction, e.g., focusing on an experimental validation of these results would be of great value.

#### 3.2.3. Temperature

The effect of temperature on breakage is twofold: on one hand it increases the particles thermal energy, thus increasing the breakup likelihood (as seen for instance in the case of protein fibrils) [74]. On the other hand, a temperature increase might induce neighboring particles in a cluster to coalesce, leading to a stronger particle–particle bond, thus diminishing the breakup rate. These aspects will be further discussed in Section 3.3.

### 3.3. Cluster coalescence

Coalescence can be referred to as liquid droplet coalescence (e.g., in emulsions) or as particle coalescence (e.g., in polymer suspensions or metal oxide aerosols). In the former case, when droplets are close enough, they fuse almost instantaneously once the liquid film (from the continuous phase) between them has been drained and the droplet film is ruptured [73], thus leading to spherical particles characterized by $d_f = 3$. In the case of polymer suspensions and aerosols instead, coalescence occurs between adjacent particles embedded in the same cluster. In other words, particles first aggregate into clusters and only subsequently neighboring particles in the aggregate start to coalesce if they are soft enough. This happens for polymer particles with a glass transition temperature ($T_g$) smaller than the operating temperature ($T_g < T$), and for metal oxide aerosols with the melt temperature ($T_m$) smaller than the operating one $T_m < T$. For both polymer particles and metal oxides, it's the interplay between the characteristic time of aggregation ($\tau_A$), of coalescence ($\tau_C$) and of the entire process ($\tau_P$) that regulates the resulting $d_f$ of the formed clusters [75]. In particular, the characteristic times for stagnant DLCA aggregation and coalescence are defined as follows:

$$\tau_C = \frac{R_P\eta_P}{\sigma_P} \tag{19}$$

$$\tau_A = \frac{3\eta_C}{8k_BTC_{part}} \tag{20}$$

where $R_P$ is the particle radius, $\eta_P$ is the particle viscosity, $\eta_C$ is the continuous phase viscosity, $\sigma_P$ is the particle surface tension, $T$ is the temperature, $k_B$ is the Boltzmann constant, and $C_{part}$ the particle concentration. Introducing then the ratio of the latter two characteristic times,

$$N = \frac{\tau_C}{\tau_A} \tag{21}$$

and recalling that $\tau_P > \tau_A$ (otherwise no aggregation would occur), it is possible to identify 3 limiting situations,

i) $N << 1$ complete, instantaneous coalescence occurs and the process evolves like in a liquid/liquid dispersion
ii) $N \approx 1$ rather compact and coalesced clusters are formed
iii) $N >> 1$, two sub-cases have to be distinguished:

a. $\tau_P < \tau_C$ no coalescence occurs (the process is too slow) and open clusters are formed, such as the ones described in the previous sections
b. $\tau_P > \tau_C$ coalescence occurs slowly and partially coalesced clusters are formed after aggregation is completed, so that eventually partially coalesced clusters are formed.

Despite the apparent simplicity of this picture, things get much more complicated when considering that these particle–particle processes occur throughout the whole cluster, and that the cluster is potentially undergoing also growth and breakage at the same time. A quantification of the characteristic time of coalescence is still far from being cluster mass specific and does not account for the presence and role of steric surfactant or charges relocation.

*3.3.1. Direct effect*

Coalescence per se, increases the fractal dimension of the clusters as the particles belonging to one aggregate start to interpenetrate and if sufficient time is left to the system, fully spherical aggregates are eventually retrieved [76].

*3.3.2. Indirect effect*

*3.3.2.1. Surface rearrangement.* When charge-stabilized polymeric particles undergo coalescence in an aggregate, a stabilization of the clusters is observed. This is related to the coalescence extent, whose increase causes a decrease of the clusters collision radii (therefore a reduced aggregation rate) and a decrease in the total surface area (decreased phase separation driving force). At the same time, a partial loss of fixed charges is observed at the particles surface due to their burying in the coalesced portion of the two particles. This means that the resulting coalesced clusters become more stable upon coalescence, but not to the extent one would expect if all charges were accumulating at the surface. Coalescence leads, as a net result, to a stability gain of the system. It is therefore possible, under appropriate conditions, to observe a switch in the aggregation mechanism from DLCA to RLCA, leading to a corresponding change in the clusters $d_f$ [77].

*3.3.2.2. Effective volume fraction and aggregation mechanism.* An increase in occupied volume fraction increases the $d_f$ of DLCA aggregating, non-coalescing particles in stagnant conditions [49], as already discussed in Section 3.1.3. In a scenario where high-concentrated, coalescing, primary particles were to aggregate, an even higher $d_f$ is expected to be observed. Besides the obvious increase due to coalescence itself, it is the large number of contact points between particles in a compact clusters that makes the difference. An increased number of neighboring particles guarantees a faster particle interpenetration and therefore a faster coalescence. The same concept holds when the initially formed clusters are obtained under aggregation regimes leading to compact clusters. For instance, aggregates formed under ballistic particle–cluster aggregation (BPCA, $d_f \approx 2.8$) will reach a fully coalesced state much faster than clusters obtained in diffusion limited cluster aggregation (DLCA, $d_f \approx 1.8$), as on average the number of nearest neighbors in the DLCA case is much lower than in the BPCA case [76,78].

*3.3.2.3. Breakup decrease due to partial coalescence.* Coalescence has an important indirect effect on the $d_f$ of clusters formed under shear conditions, as it changes the interplay between cluster aggregation and breakage, described in Section 3.2. As a matter of fact polymeric particles undergoing coalescence experience an entanglement of polymeric chains belonging to different particles, resulting in an enhanced particle–particle bond. Such link reduces the breakage likelihood and leads, somehow surprisingly, to more open clusters as compared to non-coalescing systems. It is worth noting that in this context, coalescence drives the system toward a faster gelation. Only in the case of significant/full coalescence, gelation is fully prevented as the reduced breakage is compensated by the smaller increase in occupied volume fraction (cf. Section 4).

*3.3.3. T/Tg*

Coalescence extent may be tuned by changing the operating temperature, $T$. In particular, by increasing $T$ beyond $T_g$, the polymer particles become softer and a more significant coalescence takes place, while decreasing the temperature the opposite effect is observed. Note that in Eq. (19), the particle interfacial tension $\sigma_P$ is less sensitive to temperature than the particles viscosity $\eta_{lP}$, thus leading to a characteristic coalescence time, $\tau_C$, which decreases with temperature.

*3.3.4. Surface tension*

As shown in Eq. (19), the coalescence characteristic time is also affected by the particles surface tension. This parameter reflects the intensity of the driving force toward coalescence and depends on the particles material properties and their interaction with the surrounding continuous phase. Hence, the particle surface composition is of paramount influence. It has indeed been shown experimentally [79,80] that the type of charged surface "decoration" and dispersant composition affect significantly the coalescence rate of fractal clusters consisting of soft particles. Increasing the surface charge (by deprotonation of fixed carboxylic groups for example) leads to more open clusters than in the protonated state. Such an effect has been attributed to the accumulation of fixed charges on the surface, limiting the coalescence rate. These findings should encourage colloid scientists to consider the "surface tension" of the particles as a variable that can be strongly affected by the detailed composition of the particle surface and by the dispersant, rather than as a constant value depending only on the particle material.

*3.4. Overview*

A scheme attempting to summarize the complex variable interactions discussed in this section, is shown in Fig. 4.

Fig. 4 indicates qualitatively the changes in $d_f$ from the ideal case of clusters obtained in stagnant DLCA aggregation in diluted conditions as a function of various variables (increasing along the arrows directions). In other words, when attractive forces (here electrostatic ones) and primary particle size or polydispersity are increased, the $d_f$ tends to decrease. If primary particle concentration, repulsive forces, or breakage increase, a larger $d_f$ is found (while primary particles maintain their identity). On the other hand, when coalescence occurs, an increase of $d_f$ is observed along with "molten" clusters, and primary particles lose their identity. Notably, the reported values of $d_f$ in Fig. 4 are limiting values and intermediate values are more typically observed. Despite the complex interplay between $d_f$ and the reported variables, fractal clusters have been proved useful in several different applications, which are outlined in Section 4. On the other hand, as the picture is far from being complete, exciting research directions and challenges still exist in this field, as discussed in Section 5.

## 4. Relevance of the fractal concept in colloid science

The fractal concept becomes of relevance in any type of process where colloidal particles aggregate and organize in clusters. If the concentration is high enough, the clusters start to interconnect with one another and the colloidal system may percolate. This means that a "super-cluster" spanning throughout the whole reactor/vessel, i.e., changing from a nano/micro- to a macroscale, is formed. This process is referred to as gelation and turns a "liquid-like" system into a "gel-like" one; in other words, the viscosity of the system diverges. To better visualize this, it is enough to recall that in any aggregating system

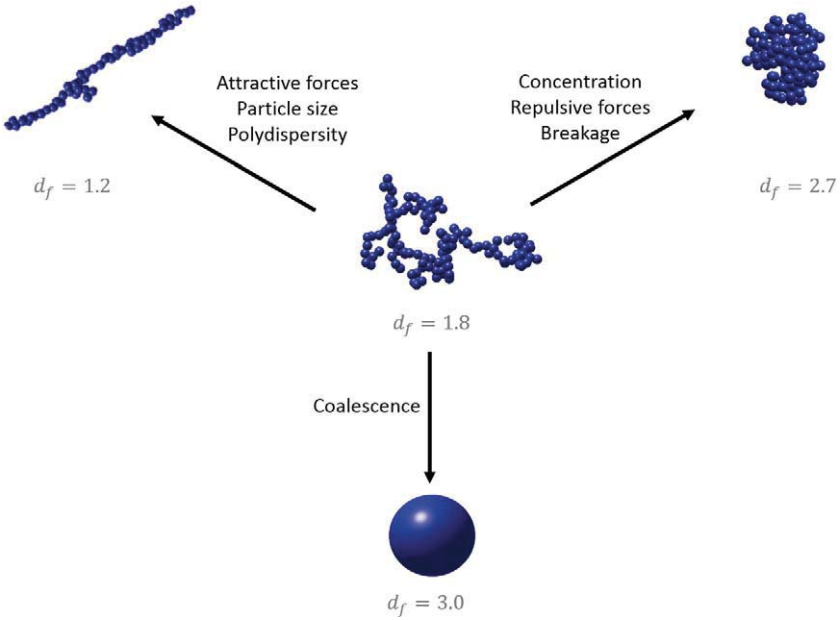


**Fig. 4.** Variables affecting the cluster structure and the corresponding fractal dimension.

the suspension viscosity progressively increases along with the occupied volume fraction $\varphi$, defined as [20]:

$$\varphi = \sum_{i=1}^{\infty} N_i \frac{4}{3}\pi R_{g,i}^3 \tag{22}$$

where $N_i$ is the concentration of clusters of size $i$, while $R_{g,i}$ is their gyration radius. Note that for the system viscosity to diverge and not only increase, gelation (i.e., percolation) has to occur; this happens when $\varphi \to \varphi_{crit}$ (e.g., $\varphi_{crit} = 0.63$ for monodisperse hard spheres in random close packing) [81]. To appreciate the link between fractal dimension and gelation, it is sufficient to substitute Eq. (1) into Eq. (22) and assume that the concentration of clusters of size $N_i$ is a function of the initial primary particle concentration $N_0$ and the average cluster size $\langle i \rangle$, i.e., $N_i \approx \frac{N_0}{\langle i \rangle}$:

$$\varphi \propto \frac{N_0}{\langle i \rangle}\langle i \rangle^{3/d_f} = N_0 \langle i \rangle^{(3-d_f)/d_f} \tag{23}$$

From Eq. (23), it is clear that the fractal dimension of the aggregating clusters regulates the gelation process: only when $d_f = 3$, i.e., only when the newly formed clusters are dense spheres, the occupied volume fraction remains constant. Whenever a porous cluster with $d_f < 3$ is formed, an increase in the occupied volume fraction is observed and when $\varphi \to \varphi_{crit}$, gelation occurs.

In the most general sense, the aggregation/gelation process can be either undesired, e.g., in industrial processes where it causes the formation of undesired macroscopic material (e.g., coagulum), or required, for instance when the obtained fractal clusters or the fractal gel is the desired product, as discussed in the following sections.

### 4.1. Coagulum formation in industrial production units

An industrially relevant process where the aggregation of colloidal particles and in particular their fractal dimension is critical is represented by heterogeneous polymerization (i.e., suspension or emulsion), typically conducted at high occupied volume fractions of polymer particles ($\varphi > 40\%$). During the reaction, the polymer particles are mechanically stirred and are therefore exposed to shear. If the energy introduced into the system is enough to overcome the particles repulsive barrier, aggregation of the primary particles may occur very abruptly and in some cases result in the percolation of the system, thus leading to the formation of macroscopic pieces of gel or coagulum [82]. In the case of coalescing systems, the aggregates evolve toward dense spheres (objects having a $d_f \to 3$). This way, even if aggregation occurs to a significant extent, coagulum formation is avoided as the occupied volume fraction and therefore the viscosity of the suspension remains constant (cf. Eq. (23)), thus preventing percolation/gelation to occur [83].

Another example of the $d_f$ impact on the operation stability of industrial units, is represented by product or by-product crystallization in microreactors, which leads to reactor clogging, of particular importance given the small reactor diameter (in the range of 10–1000 μm) [84]. The fractal dimension of the formed crystals plays a key role in this process as a low $d_f$ will cause a faster clogging. Environmental and operative parameters affect the crystal shape. For instance, it is known that low supersaturation drives the $d_f$ toward low values, while high supersaturation results in rather compact crystal structures [85]. Similar considerations hold also in the industrial production of protein-based drugs. The undesired aggregation of therapeutic proteins, which can lead to different aggregate morphologies, is a major issue that may compromise productivity, and drug safety and efficacy [86].

Another scenario where aggregates may cause severe issues is the transportation of methane in deep sea pipelines. In the typical operating conditions (about 200 atm and 2–6 °C), ice-like solids trap methane molecules forming the so-called clathrate hydrates [87]. Such hydrates can aggregate and lead to the clogging and rupture of the pipeline, with an obvious drastic ecological and economical aftermath [88].

### 4.2. Impact of fractals on material properties

By taking advantage of the fractal structure of the clusters formed by aggregation, it is possible to develop structured materials from colloidal suspensions [24]. This approach gives the possibility to functionalize small and well controllable "building blocks" (e.g., the primary particles) and use them for the build-up of more complex structures through a controlled aggregation or gelation process. In a more general sense, fractal structures strongly affect material properties; in this section, the importance of controlling the fractal dimension of such aggregates is briefly sketched with reference to some relevant application fields.

*4.2.1. Chromatography stationary phases*

Chromatography packing materials are required to have a very large surface area and specific surface properties according to the separation to be carried out. A process named reactive gelation [89] allows the preparation of such materials in 3 steps: (1) synthesis of nanoparticles functionalized with the desired moiety, (2) destabilization of the nanoparticles through salt addition forming a weak gel, (3) post-polymerization of the obtained gel by addition of monomer and initiator to increase the gel "strength." Controlling the fractal dimension of the obtained gel is a property of key importance: a low fractal dimension implies a large surface area and therefore better separation efficiency, while fulfilling the condition of a low backpressure. This procedure has been recently shown to provide materials with sufficiently large macroporority to allow perfusive convective flow, a property of particular interest for chromatographic protein purification. By taking advantage of the open fractal structure, when considering a column packed with this material, the convective flow goes within the particles. This reduces the diffusion path that the adsorbate have to cover from the particle site to the pore size, i.e., by a factor of about $10^2$. This has an obvious impact on the efficiency and therefore on the economics of the separation process [90].

*4.2.2. Filtration enhancement*

Another type of separation is filtration, where solid particles are separated from the liquid phase they are suspended in. To enhance this process, the suspended particles are typically destabilized in order to form aggregates with an improved sedimentation rate and filtration ease as compared to the primary particles. In this frame, it would be desirable to obtain rather compact aggregates ($d_f \to 3$), as such clusters exhibit a lower drag (and hence a faster sedimentation) as compared to their equally sized, more open counterparts. For this, an increased cluster compactness (i.e., with a larger $d_f$) is typically obtained by destabilizing the system in the presence of shear forces [91].

*4.2.3. Heat exchangers and insulating materials*

The addition of solid particles to a fluid is known to affect its thermal transport properties. For example, this strategy has been recently implemented in heat exchanger devices, by adding an aqueous suspension of colloidal silica so as to obtain a stable system, ranging from the fully dispersed state up to the colloidal gel one, leading to improvements of the thermal conductivity up to 20% [92]. In this frame, open clusters (having low $d_f$) should allow a faster transport of the heat when compared to their equally sized, more compact counterparts, as a more direct heat flow through the clusters occurs.

Interestingly, using silica-based materials with a colloidal fractal structure, it is possible to achieve also a reduction of the heat transfer, relevant to the production of insulation materials. A well-known strategy in this sense involves silica aerogels, whose very low conductivity (0.012–0.020 W/m/K) is strictly connected to their high porosity (>90%) (corresponding to a low $d_f$), low density (80–200 kg/m$^3$), pore structure and small pore size, allowing them to be employed as super-insulators [93].

*4.2.4. Superhydrophobic surfaces*

A recent application of fractal aggregates has been proposed by Deng et al. [94], who used soot aggregates generated by the combustion of a candle to render surfaces superamphiphobic. The superamphiphobicity is due to the intrinsic fractal structure generated by the combustion process, coupled to the hydrophobized silica coating that the authors deposed on this surface. The fractal structure helps creating tiny air pockets, which render unfavorable the penetration of a liquid, thus rendering the surface non-wettable by both water and oil.

*4.2.5. Food products*

Fractal structures are relevant also in the food industry, where protein aggregates are often employed to tune the viscosity of products. In particular, fibrillary like aggregates ($d_f \to 1$) significantly increase the viscosity of the suspension even at low protein volume fractions, while dense spherical aggregates ($d_f \to 3$) have a smaller impact on viscosity even at higher volume fractions [95]. Moreover, the same protein can lead to different structures (i.e., rods, spheres or branched, flexible strands) according to the environmental conditions employed (pH, ionic strength, protein concentration), as in the case of the whey protein isolate or beta-lactoglobulin [96]. Controlling size and shape of protein aggregates is of key importance as for instance the presence of micron-sized globular aggregates results in a coarse mouth feeling texture [95].

*4.2.6. Biomaterials*

The possibility of employing protein aggregates as biomaterials has been considered due to the intriguing combination of biocompatibility and mechanical properties they exhibit [97,98]. A relevant example in this sense is the silk protein sericin, whose self-assembly can be directed toward objects having different fractality (such as nanofibrils, hydrogels or films) by properly changing environmental (i.e., solvent) conditions [99]. Given a good control on the aggregate structure, it can be envisaged how different classes of protein-based biomaterials will represent an interesting direction for both research and industrial applications.

## 5. Possible research directions and challenges

*5.1. Link between colloidal dispersion and fractal dimension*

*Key question: Which operating parameter combination (particles size, surface properties, occupied volume fraction, shear, etc.) leads to which fractal dimension?*

The fractal structure obtained from a monodisperse colloidal suspension is a function of several operational and particle-related parameters, as discussed in Section 3. Despite the impact of some of these variables is well known, their interplay is rather complex and not fully explored. For instance, increasing the occupied volume fraction increases the $d_f$, whereas screening the electrostatic interactions upon salt addition typically reduces $d_f$. The question would then be in which conditions does one or the other phenomenon prevail and to which extent. A more quantitative link between the suspension properties and the resulting fractal structure would be of great help to design materials with porosity tailored for specific applications. Such a link is still not understood also in the case of protein structures, characterized by an even higher degree of complexity as compared to the classical colloidal particles, as it appears immediately obvious when considering hydrophobic patches, secondary and tertiary structure, denaturation, etc.

*5.2. Link between nanoscale and macroscale properties*

*Key question*: *Which are the physical properties (e.g., thermal conductivity, mechanical resistance, etc.) of a given fractal cluster*?

The idea of creating macroscopic materials starting from smaller "building blocks" is indeed a fascinating idea and a few examples are found in the literature [89,100]. In this respect, there are still several conceptual points that are worth investigating, such as for example, establishing the link between the nanoscale properties (of the nanoparticles used as building blocks) with the macroscopic objects (created starting from those nanoparticles). For instance, it would be desirable to predict the conductivity or the mechanical resistance of a cluster given its fractal dimension. In this context, of course whether or not the primary particles percolate at the scale of the macroscopic object plays a fundamental role.

*5.3. Fractal dimension in heteroaggregation*

*Key question*: *Which is the fractal dimension resulting from the stagnant and shear heteroaggregation*?

Fractal clusters exhibiting multiple properties (e.g., conductivity and mechanical stability) can be prepared employing two (or more) distinct types of colloidal particles in a heteroaggregation process. The different colloidal particles usually differ in terms of chemical composition, size, and surface properties. While there is a relative clarity in terms of how to deal with the interaction potential of two different types of particles [101,102], the effect of particle size on the fractal dimension of heteroclusters is less explored, with some noteworthy exceptions [26]. On the other hand, there are very limited experimental insights in this sense, whereas it would be interesting to explore the fractal dimension of clusters obtained in binary aggregation in both stagnant and shear condition. Shear-induced aggregation especially is a very promising methodology to produce the aforementioned hetero-materials in an economically and industrially feasible way. This would in fact provide a tool where different materials (organic and inorganic) could be mixed at the nanoscale in the form of suspensions and later aggregated in fractal clusters made of different materials. This would represent an alternative to the current extrusion processes where the different materials are forced to mix by introducing energy to the system through heat and shear. In this case entropy would be used to mix colloidal suspensions. In this context, of specific interest is again the fractal geometry and its ability to create percolating structures. An interesting result in this direction has been reported by Varrato et al. in demonstrating the possibility of creating bigels structures using DNA [103].

### 5.4. Anisotropic particles

*Key questions*: *How is anisotropy* (*in terms of shape and surface properties*) *affecting the aggregate structure*? *Which anisotropic particles can be used as a reliable model systems for protein aggregation*?

Particles exhibiting any degree of asymmetry, may this be in shape, surface (e.g., presence of patches), complex architectures (e.g., *Janus* particles), or in compartmentalization (e.g., core-shell particles) are termed anisotropic [104]. Notably, the aggregation of anisotropic particles is extremely complex and requires the consideration of additional parameters otherwise typically ignored, such as the aspect ratio, whose increase was shown to lead to an increase in fractal dimension [105]. On the other hand, provided that these particles are properly synthesized, very well-defined and peculiar structures can be obtained from their aggregation, opening up interesting possibilities for the preparation of materials [106]. Moreover, studying the clustering of such anisotropic particles might shed light on the behavior of other complex systems; the aggregation of patchy spheres might for instance be a good model system for investigating protein aggregation, able to mimic and possibly explain the role of the hydrophobic/hydrophilic protein domains.

## 6. Closing comment

A future where fractal structures can be designed by controlling aggregation with a nanometer precision is probably still far, but the times are mature for deepening the underlying physical understanding and the available degrees of freedom, in a view to control and tune cluster fractality. This in fact has the potential to change our way to think, create and produce new structured materials.

## Acknowledgments

S.L. gratefully acknowledges the Swiss National Science Foundation (SNSF) for financial support (grant number P2EZP2_159128). M.L. also gratefully acknowledges SNSF for financial support (grants number PP00P2133597/1 and PP00P2_159258). M.M. also gratefully acknowledges SNSF for financial support (grant number 200020_147137/1).

## References

[1] Cosgrove T. Colloid Science Principles, Methods and Applications. 2nd ed. Chichester, U.K.: Wiley; 2010
[2] Lu PJ, Weitz DA. Colloidal particles: crystals, glasses, and gels. Annu Rev Conden Ma P 2013;4:217–33.
[3] Forrest SR, Witten TA. Long-range correlations in smoke-particle aggregates. J Phys A Math Gen 1979;12 [L109-L17].
[4] Friedlander SK. Smoke, Dust, and Haze Fundamentals of Aerosol Dynamics. 2nd ed. New York: Oxford University Press; 2000.
[5] Sorensen CM, Roberts GC. The prefactor of fractal aggregates. J Colloid Interface Sci 1997;186:447–52.
[6] Gmachowski L. Calculation of the fractal dimension of aggregates. Colloids Surf A Physicochem Eng Asp 2002;211:197–203.
[7] Knowles TP, Fitzpatrick AW, Meehan S, Mott HR, Vendruscolo M, Dobson CM, et al. Role of intermolecular forces in defining material properties of protein nanofibrils. Science 2007;318:1900–3.
[8] Weitz DA, Oliveria M. Fractal structures formed by kinetic aggregation of aqueous gold colloids. Phys Rev Lett 1984;52:1433–6.
[9] Gauer C, Wu H, Morbidelli M. Control of coalescence in clusters of elastomer colloids through manipulation of polymer composition. Macromolecules 2009;42: 9103–10.
[10] Lattuada M, Wu H, Morbidelli M. Hydrodynamic radius of fractal clusters. J Colloid Interface Sci 2003;268:96–105.
[11] Sorensen CM. The mobility of fractal aggregates: a review. Aerosol Sci Tech 2011; 45:765–79.
[12] Lattuada M, Wu H, Morbidelli M. A simple model for the structure of fractal aggregates. J Colloid Interface Sci 2003;268:106–20.
[13] IUPAC. Definition of coagulation
[14] Bushell GC, Yan YD, Woodfield D, Raper J, Amal R. On techniques for the measurement of the mass fractal dimension of aggregates. Adv Colloid Interface 2002;95:1–50.
[15] Mezzenga R, Fischer P. The self-assembly, aggregation and phase transitions of food protein systems in one, two and three dimensions. Rep Prog Phys 2013;76.
[16] Sorensen CM. Light scattering by fractal aggregates: a review. Aerosol Sci Tech 2001;35:648–87.
[17] Berne BJ, Pecora R. Dynamic Light Scattering: With Applications to Chemistry, Biology, and Physics. Dover ed. Mineola, N.Y.: Dover Publications; 2000
[18] Johnson CS, Gabriel DA. Laser Light Scattering. New York: Dover; 1994.
[19] Wu H, Lattuada M, Sandkuhler P, Sefcik J, Morbidelli M. Role of sedimentation and buoyancy on the kinetics of diffusion limited colloidal aggregation. Langmuir 2003; 19:10710–8.
[20] Berg JC. An Introduction to Interfaces and Colloids the Bridge to Nanoscience. Hackensack: World Scientific; 2010.
[21] Oh C, Sorensen CM. The effect of overlap between monomers on the determination of fractal cluster morphology. J Colloid Interface Sci 1997;193:17–25.
[22] Ehrl L, Soos M, Lattuada M. Generation and geometrical analysis of dense clusters with variable fractal dimension. J Phys Chem B 2009;113:10587–99.
[23] IUPAC. Definition of colloidal gel.
[24] Wu H, Morbidelli M. A model relating structure of colloidal gels to their elastic properties. Langmuir 2001;17:1030–6.
[25] Dickinson E. Structure and rheology of colloidal particle gels: insight from computer simulation. Adv Colloid Interface 2013;199:114–27.
[26] Eggersdorfer ML, Pratsinis SE. The structure of agglomerates consisting of polydisperse particles. Aerosol Sci Tech 2012;46:347–53.
[27] Hutter M. Coagulation rates in concentrated colloidal suspensions studied by Brownian dynamics simulation. Phys Chem Chem Phys 1999;1:4429–36.
[28] Whittle M, Dickinson E. Brownian dynamics simulation of gelation in soft sphere systems with irreversible bond formation. Mol Phys 1997;90:739–57.
[29] Dickinson E. Structure and rheology of simulated gels formed from aggregated colloidal particles. J Colloid Interface Sci 2000;225:2–15.
[30] Buesser B, Grohn AJ, Pratsinis SE. Sintering rate and mechanism of TiO2 nanoparticles by molecular dynamics. J Phys Chem C 2011;115:11030–5.
[31] Kryven I, Lazzari S, Storti G. Population balance modeling of aggregation and coalescence in colloidal systems. Macromol Theory Simul 2014;23:170–81.
[32] Ramkrishna D. Population balances theory and applications to particulate systems in engineering. San Diego: Academic Press; 2000.
[33] Lin MY, Lindsay HM, Weitz DA, Ball RC, Klein R, Meakin P. Universality in colloid aggregation. Nature 1989;339:360–2.
[34] Mellema M, van Opheusden JHJ, van Vliet T. Relating colloidal particle interactions to gel structure using Brownian dynamics simulations and the Fuchs stability ratio. J Chem Phys 1999;111:6129–35.
[35] Meakin P. Fractal aggregates. Adv Colloid Interface 1988;28:249–331.
[36] Hutter M. Local structure evolution in particle network formation studied by Brownian dynamics simulation. J Colloid Interface Sci 2000;231:337–50.
[37] Kim AY, Berg JC. Fractal aggregation: scaling of fractal dimension with stability ratio. Langmuir 2000;16:2101–4.
[38] Meakin P, Jullien R. The effects of restructuring on the geometry of clusters formed by diffusion-limited, ballistic, and reaction-limited cluster cluster aggregation. J Chem Phys 1988;89:246–50.
[39] Heinson WR, Pierce F, Sorensen CM, Chakrabarti A. Crossover from ballistic to Epstein diffusion in the free-molecular regime. Aerosol Sci Tech 2014;48:738–46.
[40] Kim AY, Hauch KD, Berg JC, Martin JE, Anderson RA. Linear chains and chain-like fractals from electrostatic heteroaggregation. J Colloid Interface Sci 2003;260: 149–59.
[41] Lu PJ, Conrad JC, Wyss HM, Schofield AB, Weitz DA. Fluids of clusters in attractive colloids. Phys Rev Lett 2006;96.

[42] Yang YJ, Kelkar AV, Zhu X, Bai G, Ng HT, Corti DS, et al. Effect of sodium dodecylsulfate monomers and micelles on the stability of aqueous dispersions of titanium dioxide pigment nanoparticles against agglomeration and sedimentation. J Colloid Interface Sci 2015;450:434–45.
[43] Halsey TC. Electrorheological fluids. Science 1992;258:761–6.
[44] de Vicente J, Klingenberg DJ, Hidalgo-Alvarez R. Magnetorheological fluids: a review. Soft Matter 2011;7:3701–10.
[45] Furlan M, Lattuada M. Fabrication of anisotropic porous silica monoliths by means of magnetically controlled phase separation in sol–gel processes. Langmuir 2012; 28:12655–62.
[46] Degennes PG, Pincus PA. Pair correlations in a ferromagnetic colloid. Phys Kondensiterten Mater 1970;11 [189 − +].
[47] Tavares JM, Weis JJ, da Gama MMT. Quasi-two-dimensional dipolar fluid at low densities: Monte Carlo simulations and theory. Phys Rev E 2002;65.
[48] Vutukuri HR, Demirors AF, Peng B, van Oostrum PDJ, Imhof A, van Blaaderen A. Colloidal analogues of charged and uncharged polymer chains with tunable stiffness. Angew Chem Int Ed 2012;51:11249–53.
[49] Gonzalez AE, Martinez-Lopez F, Moncho-Jorda A, Hidalgo-Alvarez R. Concentration effects on two- and three-dimensional colloidal aggregation. Phys A 2002;314: 235–45.
[50] Wu H, Lattuada M, Morbidelli M. Dependence of fractal dimension of DLCA clusters on size of primary particles. Adv Colloid Interface Sci 2013;195:41–9.
[51] Nicoud L, Lattuada M, Yates A, Morbidelli M. Impact of aggregate formation on the viscosity of protein solutions. Soft Matter 2015.
[52] Bushell G, Amal R. Fractal aggregates of polydisperse particles. J Colloid Interface Sci 1998;205:459–69.
[53] Tence M, Chevalier JP, Jullien R. On the measurement of the fractal dimension of aggregated particles by electron-microscopy—experimental-method, corrections and comparison with numerical-models. J Phys Paris 1986;47:1989–98.
[54] Robinson DJ, Earnshaw JC. Long-range order in 2-dimensional fractal aggregation. Phys Rev Lett 1993;71:715–8.
[55] Moncho-Jorda A, Martinez-Lopez F, Gonzalez AE, Hidalgo-Alvarez R. Role of long-range repulsive interactions in two-dimensional colloidal aggregation: experiments and simulations. Langmuir 2002;18:9183–91.
[56] Meakin P. Diffusion-controlled aggregation on two-dimensional square lattices—results from a new cluster-cluster aggregation model. Phys Rev B 1984; 29:2930–42.
[57] Earnshaw JC, Robinson DJ. Scale-invariance in 2-dimensional reaction-limited colloidal aggregation. J Phys Condens Matter 1995;7:L397–403.
[58] Thill A, Spalla O. Aggregation due to capillary forces during drying of particle submonolayers. Colloids Surf A Physicochem Eng Asp 2003;217:143–51.
[59] Biggs S, Habgood M, Jameson GJ, Yan YD. Aggregate structures formed via a bridging flocculation mechanism. Chem Eng J 2000;80:13–22.
[60] Zhou Y, Franks GV. Flocculation mechanism induced by cationic polymers investigated by light scattering. Langmuir 2006;22:6775–86.
[61] Li T, Zhu Z, Wang DS, Yao CH, Tang HX. Characterization of floc size, strength and structure under various coagulation mechanisms. Powder Technol 2006;168: 104–10.
[62] Yu JF, Wang DS, Ge XP, Yan MQ, Yang M. Flocculation of kaolin particles by two typical polyelectrolytes: a comparative study on the kinetics and floc structures. Colloids Surf A Physicochem Eng Asp 2006;290:288–94.
[63] Gonzalez AE. Colloidal aggregation with sedimentation: computer simulations. Phys Rev Lett 2001;86:1243–6.
[64] Gonzalez AE. Colloidal aggregation in the presence of a gravitational field. J Phys Condens Matter 2002;14:2335–45.
[65] Allain C, Cloitre M, Wafra M. Aggregation and sedimentation in colloidal suspensions. Phys Rev Lett 1995;74:1478–81.
[66] Conchuir BO, Zaccone A. Mechanism of flow-induced biomolecular and colloidal aggregate breakup. Phys Rev E 2013;87.
[67] Eggersdorfer ML, Kadau D, Herrmann HJ, Pratsinis SE. Fragmentation and restructuring of soft-agglomerates under shear. J Colloid Interface Sci 2010;342: 261–8.
[68] Zaccone A, Soos M, Lattuada M, Wu H, Babler MU, Morbidelli M. Breakup of dense colloidal aggregates under hydrodynamic stresses. Phys Rev E 2009;79.
[69] Conchuir BO, Harshe YM, Lattuada M, Zaccone A. Analytical model of fractal aggregate stability and restructuring in shear flows. Ind Eng Chem Res 2014;53:9109–19.
[70] Shih WY, Liu J, Shih WH, Aksay IA. Aggregation of colloidal particles with a finite interparticle attraction energy. J Stat Phys 1991;62:961–84.
[71] Fernandez-Nieves A, Fernandez-Barbero A, Vincent B, de las Nieves FJ. Reversible aggregation of soft particles. Langmuir 2001;17:1841–6.
[72] Ren Z, Harshe YM, Lattuada M. Influence of the potential well on the breakage rate of colloidal aggregates in simple shear and uniaxial extensional flows. Langmuir 2015;31:5712–21.
[73] Ottino JM, DeRoussel P, Hansen S, Khakhar DV. Mixing and dispersion of viscous liquids and powdered solids. In: James W, editor. Advances in chemical engineering. Academic Press; 1999. p. 105–204.
[74] Nicoud L, Lazzari S, Barragan DB, Morbidelli M. Fragmentation of amyloid fibrils occurs in preferential positions depending on the environmental conditions. J Phys Chem B 2015;119:4644–52.
[75] Lazzari S, Jaquet B, Colonna C, Storti G, Lattuada M, Morbidelli M. Interplay between aggregation and coalescence of polymeric particles: experimental and modeling insights. Langmuir 2015;31(34):9296–305.
[76] Eggersdorfer ML, Kadau D, Herrmann HJ, Pratsinis SE. Multiparticle sintering dynamics: from fractal-like aggregates to compact structures. Langmuir 2011;27: 6358–67.
[77] Gauer C, Wu H, Morbidelli M. Reduction of surface charges during coalescence of elastomer particles. J Phys Chem B 2010;114:8838–45.
[78] Mandelbrot BB. The Fractal Geometry of Nature (Formerly: Fractals). (ed. 1983), updated &an augm. ed. New York: Freeman; 1983.
[79] Gauer C, Wu H, Morbidelli M. Coalescence control of elastomer clusters by fixed surface charges. J Phys Chem B 2010;114:1562–7.
[80] Gauer C, Wu H, Morbidelli M. Effect of surface properties of elastomer colloids on their coalescence and aggregation kinetics. Langmuir 2009;25:12073–83.
[81] Bicerano J, Douglas JF, Brune DA. Model for the viscosity of particle dispersions. J Macromol Sci R M C 1999;C39:561–642.
[82] Zaccone A, Wu H, Gentili D, Morbidelli M. Theory of activated-rate processes under shear with application to shear-induced aggregation of colloids. Phys Rev E 2009;80.
[83] Lazzari S, Maggioni GM, Soos M, Wu H, Morbidelli M. Shear-stability and gelation of inverse latexes. Soft Matter 2013;9:10866–76.
[84] Hartman RL, Naber JR, Zaborenko N, Buchwald SL, Jensen KF. Overcoming the challenges of solid bridging and constriction during Pd-catalyzed C-N bond formation in microreactors. Org Process Res Dev 2010;14:1347–57.
[85] Baldyga J, Jasinska M, Orciuch W. Barium sulphate agglomeration in a pipe—an experimental study and CFD modeling. Chem Eng Technol 2003;26:334–40.
[86] Vazquez-Rey M, Lang DA. Aggregates in monoclonal antibody manufacturing processes. Biotechnol Bioeng 2011;108:1494–508.
[87] Kvamme B, Kuznetsova T, Bauman JM, Sjoblom S, Kulkarni AA. Hydrate formation during transport of natural gas containing water and impurities. J Chem Eng Data 2016;61:936–49.
[88] Kelland MA. History of the development of low dosage hydrate inhibitors. Energy Fuel 2006;20:825–47.
[89] Marti N, Quattrini F, Butte A, Morbidelli M. Production of polymeric materials with controlled pore structure: the “reactive gelation” process. Macromol Mater Eng 2005;290:221–9.
[90] de Neuville BC, Lamprou A, Morbidelli M, Soos M. Perfusive ion-exchange chromatographic materials with high capacity. J Chromatogr A 2014;1374:180–8.
[91] Gregory J. The role of floc density in solid–liquid separation. Adv Filtr Sep Technol 1998;12(1998):405–14.
[92] Lotfizadeh S, Desai T, Matsoukas T. The thermal conductivity of clustered nanocolloids. Appl Mater 2014;2.
[93] Koebel M, Rigacci A, Achard P. Aerogel-based thermal superinsulation: an overview. J Sol-Gel Sci Technol 2012;63:315–39.
[94] Deng X, Mammen L, Butt H-J, Vollmer D. Candle soot as a template for a transparent robust superamphiphobic coating. Science 2012;335:67–70.
[95] Bouhallab S, Croguennec T. Spontaneous assembly and induced aggregation of food proteins. Adv Polym Sci 2014;256:67–101.
[96] Nicolai T, Britten M, Schmitt C. Beta-lactoglobulin and WPI aggregates: formation, structure and applications. Food Hydrocoll 2011;25:1945–62.
[97] Hardy JG, Romer LM, Scheibel TR. Polymeric materials based on silk proteins. Polymer 2008;49:4309–27.
[98] Knowles TPJ, Buehler MJ. Nanomechanics of functional and pathological amyloid materials. Nat Nanotechnol 2011;6:469–79.
[99] Khire TS, Kundu J, Kundu SC, Yadavalli VK. The fractal self-assembly of the silk protein sericin. Soft Matter 2010;6:2066–71.
[100] Lu ZD, Yin YD. Colloidal nanoparticle clusters: functional materials by design. Chem Soc Rev 2012;41:6874–87.
[101] Lopez-Lopez JM, Moncho-Jorda A, Puertas AM, Schmitt A, Hidalgo-Alvarez R. Multiple time scales and cluster formation mechanisms in charge-heteroaggregation processes. Soft Matter 2010;6:3568–72.
[102] Lopez-Lopez JM, Schmitt A, Moncho-Jorda A, Hidalgo-Alvarez R. Stability of binary colloids: kinetic and structural aspects of heteroaggregation processes. Soft Matter 2006;2:1025–42.
[103] Varrato F, Di Michele L, Belushkin M, Dorsaz N, Nathan SH, Eiser E, et al. Arrested demixing opens route to bigels. Proc Natl Acad Sci U S A 2012;109:19155–60.
[104] Lee KJ, Yoon J, Lahann J. Recent advances with anisotropic particles. Curr Opin Colloid Interface Sci 2011;16:195–202.
[105] Mohraz A, Moler DB, Ziff RM, Solomon MJ. Effect of monomer geometry on the fractal structure of colloidal rod aggregates. Phys Rev Lett 2004;92.
[106] Glotzer SC, Solomon MJ. Anisotropy of building blocks and their assembly into complex structures. Nat Mater 2007;6:557–62.
[107] Pamies R, Hernandez Cifre JG, Fernandez Espin V, Collado Gonzalez MM, Diaz Baños FG. Aggregation bahavior of gold nanoparticles in saline aqueous media. J Nanopart Res 2014;16(2376):11.